4356–4364 *Nucleic Acids Research, 1998, Vol. 26, No. 19*

Transfer RNA mimicry among tymoviral genomic RNAs ranges from highly efficient to vestigial

Theo W. Dreher[1,2,*] and Joel B. Goodwin[1]

[1]Department of Microbiology and [2]Center for Gene Research and Biotechnology, Oregon State University, Corvallis, OR 97331-3804, USA

Received July 6, 1998; Revised July 31, 1998; Accepted August 11, 1998

ABSTRACT

Three tRNA-associated properties of a representative set of tymoviral RNAs have been quantitatively assessed using higher plant (wheat germ) proteins: aminoacylation, EF-1α•GTP binding, and 3′-adenylation of 3′-CC forms of the RNAs by CTP, ATP:tRNA nucleotidyltransferase. The RNAs fall into three classes differing in the extent of tRNA mimicry. Turnip yellow mosaic (TYMV) and kennedya yellow mosaic virus RNAs had activities in all three properties similar to those of a higher plant $tRNA^{Val}$ transcript, and thus are remarkable tRNA mimics. Although the isolated ~83 nt long tRNA-like structures showed high activity in these assays, in the case of TYMV, the 6318 nt long TYMV RNA was an even better substrate for valylation. Eggplant mosaic virus RNA, which has a differently constructed acceptor stem pseudoknot, differed from the above tymoviral RNAs in binding more weakly to EF-1α•GTP. Erysimum latent virus RNA, which lacks an identifiable anticodon domain, could not be valylated and had very low 3′-adenylation activity. The range of tRNA mimicry within the tymovirus genus thus ranges from extremely highly developed to minimal. The implications on the role of the tRNA mimicry in viral biology are discussed.

INTRODUCTION

The genomic RNAs of certain positive-sense RNA plant viruses possess 3′-terminal tRNA-like structures capable of aminoacylation and possessing other tRNA-like properties (1,2). Among these viruses, the tRNA mimicry of turnip yellow mosaic tymovirus (TYMV) RNA has been the most intensively studied, both from the biochemical and virological point of view. The 6.3 kb genomic TYMV RNA can be valylated to high levels *in vitro* with valyl-tRNA synthetase (ValRS) activities from bacterial, yeast, animal or plant sources (3–6). Valylated viral 3′-RNA fragments were detected after microinjection into *Xenopus* oocytes (7) and in infected Chinese cabbage tissue (8), demonstrating that valylation can occur *in vivo*. By mutating the valine identity elements shown to be present in the anticodon loop of the TYMV tRNA-like structure (TLS) (9), it was observed that genomic RNAs incapable of *in vitro* valylation failed to amplify in plant cells (10).

Genetic studies on the role of tRNA mimicry in the TYMV life cycle have suggested a role for EF-1α. TYMV genomes with methionine in place of valine identity are infectious to plants (11), indicating that aminoacylation (which leads to EF-1α binding) rather than a specific interaction with ValRS is needed to support viral amplification. The infectivity of chimeric TYMV genomes with heterologous 3′-termini incapable of *in vitro* aminoacylation by wheat germ aminoacyl-tRNA synthetases (12) has led to the model that EF-1α binding negatively regulates minus strand viral RNA synthesis. The properties of various infectious TYMV genomes (11,12) are inconsistent with an alternative role for EF-1α as a transcription factor involved in assembling a pre-initiation polymerase complex at the 3′-end of the viral RNA. This conclusion is supported by our recent demonstration that the tRNA-like structure does not act as a promoter of minus strand synthesis by TYMV RNA-dependent RNA polymerase *in vitro* (13). In the case of the chimeric, non-aminoacylatable genomes mentioned above, we postulate that the role of EF-1α has been replaced by another protein that binds the 3′-terminal region of the RNA, perhaps an aminoacyl-tRNA synthetase.

In order to fully unravel the role of the tRNA mimicry in TYMV biology, a quantitative understanding of the tRNA-like properties is essential. To date, the efficiencies of the tRNA-like properties of TYMV RNA relative to $tRNA^{Val}$ have not been quantitatively established using proteins from higher plants, the host organisms for TYMV. Using yeast ValRS, Giegé *et al.* (5) determined a k_{cat}/K_m for virion RNA of 0.04–0.06 relative to that of yeast $tRNA^{Val}$, compared to 10^{-5} or so that is typical for non-cognate tRNAs (14). Valylated TYMV RNA is known to form ternary complexes with *Escherichia coli* EF-Tu•GTP (15) and wheat germ EF-1α•GTP (16,17), but the stabilities of these complexes have not been determined. It is also known that TYMV virion RNA, which lacks the 3′-terminal adenylate residue (18), is a substrate for [CTP, ATP]:tRNA nucleotidyltransferase (CCA-NTase) from several sources (4,5,19), but again no quantitative comparisons to tRNA have been made.

*To whom correspondence should be addressed at: Department of Microbiology, Oregon State University, Corvallis, OR 97331-3804, USA. Tel: +1 541 737 1795; Fax: +1 541 737 0497; Email: drehert@bcc.orst.edu

Table 1. Deoxyoligonucleotides used as PCR primers to generate transcriptional templates

RNA transcript	Upstream (+) primer	Downstream (–) primer
TY-264	**T7**-*GGGAGA*GGGTCAAAGATTCG[a]	TGGTTCCGATGACCCTCG
TYMV-TLS	**T7**-GCTCGCCAGTT	
KYMV-TLS	**T7**-GGTCGCCAGT	TGGTCCTGGTGACGTCCA
EMV-TLS	**T7**-GGCGGACAGTT	TGGTTCCCGTTGACCCACG
SHMV-TLS	**T7**-GCCGCGAAGTC	TGGGCCCTGTATCCCCAGGGT
TY-ELV-CCCCA	**T7**-*GGGAGA*GGGTCAAAGATTCG	TGGGGTGTCCCTTTACCT
TY-ELV-CCCA	**T7**-*GGGAGA*GGGTCAAAGATTCG	TGGGTGTCCCTTTACCT
$tRNA^{Val}$ (3′-CC) tr[b]	**T7**-G	GGTGGCTTCGCCCGGACT

The DNAs used as PCR templates are indicated in the text.
[a]**T7** refers to the untranscribed part of the T7 promoter: TAATACGACTCACTATA. Nucleotides in italics are non-viral additions originating from the vector sequence.
[b]Intact $tRNA^{Val}$ (3′-CCA) was made from linearized plasmid DNA. 3′-CC variants of TY-264, TYMV-TLS, KYMV-TLS, EMV-TLS and SHMV-TLS RNAs were made using a downstream primer differing from those listed above by the omission of the 5′-T.

The genomic RNAs of several other tymoviruses have tRNA-like stuctures similar to that of TYMV RNA and have been shown to support valylation (20,21). Only an incomplete tRNA-like structure appears to be present in erysimum latent tymovirus RNA (ELV; 22), and the 3′-ELV RNA cannot be aminoacylated with wheat germ aminoacyl-tRNA synthetases (12). tRNA properties other than aminoacylation have not been investigated for tymoviral RNAs other than TYMV.

We catalogue here the quantitative tRNA mimicry of representative tymoviral RNAs using higher plant (wheat germ) proteins by direct comparison with plant $tRNA^{Val}$. These RNAs have been studied to determine the extent of conservation across the tymovirus group of tRNA mimicry, in light of its crucial role in TYMV biology. Our studies have revealed a wide continuum of tRNA mimicry among the tymoviruses, from the highly developed (TYMV, KYMV) to the vestigial (ELV). This finding is compatible with our current model that the crucial role of tRNA mimicry in the tymoviruses is simply to provide a binding site for a protein that can regulate minus strand synthesis, but less compatible with the alternative view that the TLS is involved in complex interactions promoting assembly of a minus strand initiation complex.

MATERIALS AND METHODS

Preparation of RNAs

TYMV virion RNA was prepared from Chinese cabbage leaves (cv. Spring-A1) infected with TYMC (TYMV-Corvallis) as described (23). TYMV-H virion RNA, described by Goodwin *et al.* (12), was similarly obtained.

Viral RNAs representing short 3′-fragments of the genomic RNAs were transcribed with T7 RNA polymerase from DNA templates made by PCR as described (24). Previously described clones containing cDNAs representing the TLSs of TYMV (pT7YSma; 6), KYMV (pTYMC-KYMV), EMV (pTYMC-EMV) and SHMV RNAs (formerly called CcTMV; pTYMC-CcTMV) (23), and the 3′-region of ELV (pTYMC-ELV; 12) were used as templates in the PCR reactions. The primer pairs used to generate transcriptional templates for the various RNAs are listed in Table 1; all downstream primers were purified by denaturing PAGE (20%). Conditions for PCR and transcription were as described (24), except that all RNAs other than TY-264 (formerly named TYSma) and TY-ELV were transcribed in the presence of 10 mM 5′-GMP and 1 mM GTP in order to generate 5′-monophosphate termini (25).

Substrate RNAs for 3′-adenylation assays lacked the 3′-terminal A residues shown in Figure 1. These RNAs were made from PCR-generated templates as above, using the 5′-primers indicated in Table 1 and 3′-primers related to those in Table 1, but lacking the 5′-T residue.

Transcripts (with 5′-GMP termini) corresponding to the unmodified sequence of lupine $tRNA^{Val}$ (26) were made with T7 RNA polymerase from a synthetic clone pTVAL linearized at a *Bst*NI site placed precisely at the 3′-end. Note that the resultant $tRNA^{Val}$ transcript has a -CAC- anticodon in place of the modified -IAC- (I = inosine).

Transcripts were purified by denaturing PAGE (8%), recovered by electroelution and dialyzed against water. RNA concentrations were determined spectrophotometrically, and adjusted on the basis of valylation plateaux (correction for the presence of non-templated 3′-nucleotides on ~40% of transcripts).

Aminoacylation assays

Valylation and histidylation assays were performed in TM buffer [25 mM Tris–HCl (pH 8.0), 2 mM $MgCl_2$, 1 mM ATP, 0.1 mM spermine] or in IV buffer [30 mM HEPES (*N*-2-hydroxyethylpiperazine-*N*′-ethanesulfonic acid)/KOH (pH 7.5), 100 mM potassium acetate, 2.5 mM magnesium acetate, 1.5 mM ATP] together with 10 μM [^{3}H]valine (10–25 Ci/mmol) or 10 μM [^{3}H]histidine (12 Ci/mmol) at 30°C. The partially purified aminoacyl-tRNA synthetase preparation from wheat germ, the determination of [^{3}H]amino acid incorporation, and the methods for determining kinetic parameters were as previously described (9). For kinetic parameter determinations, wheat germ ValRS (11 μg total protein/ml) was present in the concentration range in

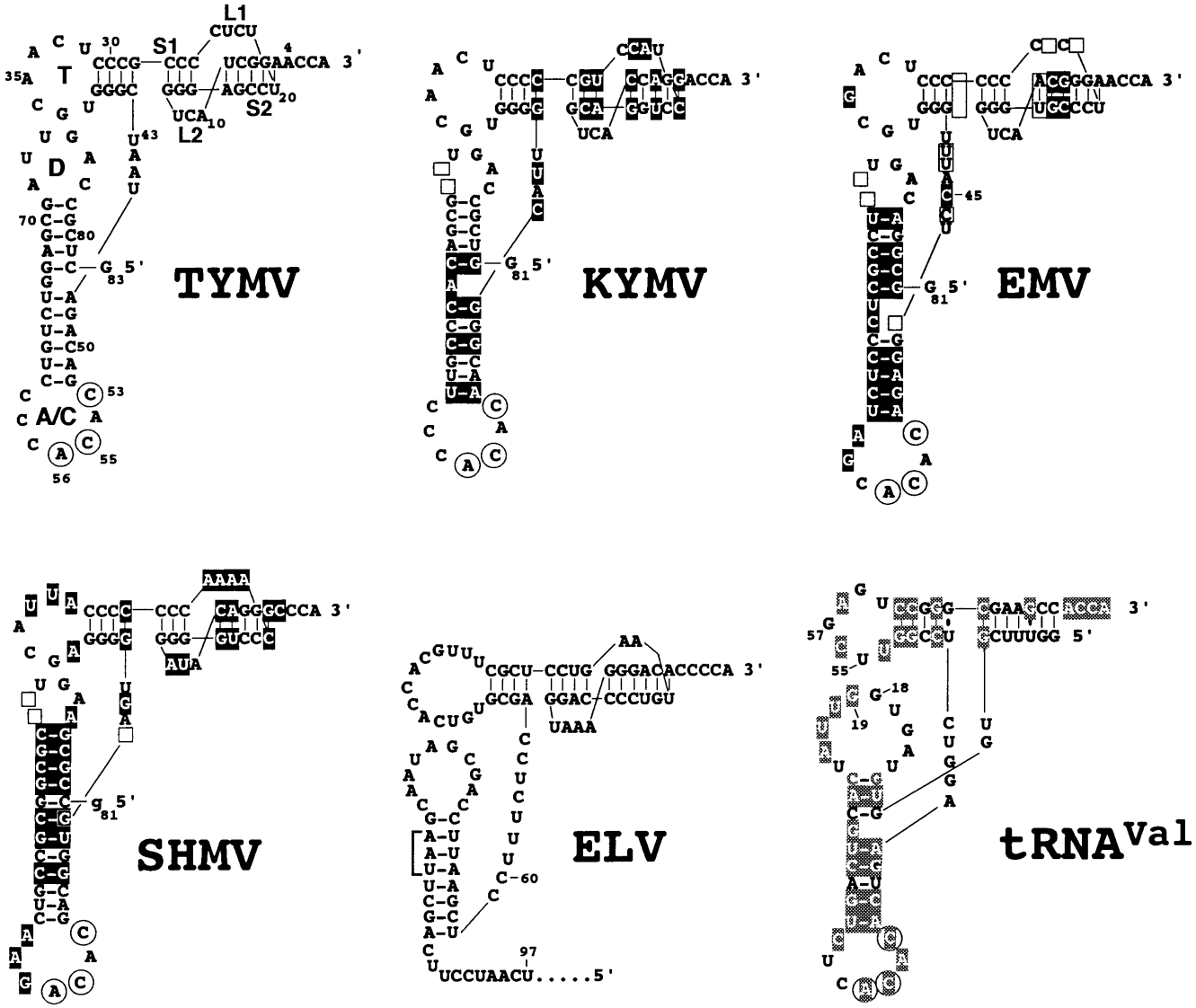

Figure 1. tRNA-like structures (TLSs) used in these studies. The TYMV-TLS is shown next to similar TLSs from the tymoviruses kennedya yellow mosaic virus (KYMV) and eggplant mosaic virus (EMV) and from the tobamovirus sunn-hemp mosaic virus (SHMV). The sequences shown correspond precisely to the TLS RNAs used in the experiments reported here; note that in the case of the SHMV TLS, the 5′ residue is shown in lower case to denote a substitution of the A present in the viral RNA with G, to permit efficient transcription with T7 RNA polymerase. Sequence differences from the TYMV-TLS are indicated by reverse-shading; deletions are marked by empty boxes and insertions by boxed nucleotides. Features of the TYMV TLS that are analogous to those of canonical tRNAs are indicated: the anticodon loop (A/C) with its valine-specific CAC anticodon, and the D-like and T-like loops. The amino acid acceptor stem is built as a pseudoknot, whose stem segments S1 and S2, and loop segments L1 and L2 are indicated. Also shown is part of the 3′-terminal region of another tymoviral RNA, that from erysimum latent virus (ELV), and a derivative of lupine tRNA^{Val} (CAC anticodon in place of IAC; I = inosine). While the structure of the TYMV-TLS has been determined experimentally, the structure shown for the ELV sequence is based on computer-assisted prediction. The ELV 3′-sequence shown was studied as part of a longer RNA, TY-ELV RNA, in which the ELV sequence was fused to the non-TLS TYMV sequences present in TY-264 (sequences upstream of TYMV nt 83, numbered from 3′-end; 23). The ELV 3′-RNA differs at nt 61 from the wild type U. The UAA codon terminating the ELV coat protein ORF is indicated with a bracket. In the tRNA^{Val} structure, nucleotide identities with TYMV RNA are marked by gray reverse shading. The valine identity elements present in the anticodon loops are circled for each RNA except ELV RNA. Note that numbering of viral RNAs is from the 3′-end.

which initial rates were proportional to enzyme concentration. Pure yeast HisRS was used in some experiments.

EF-1α binding assays

RNAs (30–50 pmol) were valylated in TM buffer as above with [^{3}H]valine (46–47 Ci/mmol; Dupont-NEN) and wheat germ ValRS for 30 min. After completion, the reactions were acidified by adjusting to 75 mM sodium acetete (pH 5.2), deproteinized with phenol/chloroform equilibrated to pH 5.2 with sodium acetete, and ethanol precipitated. After recovery by centrifugation, the valylated RNAs were redissolved in 5 mM sodium acetate (pH 5.2) and stored at –80°C until use.

Purified wheat germ EF-1α (27) was activated by incubation with 20 μM GTP in EF buffer [40 mM HEPES-KOH (pH 7.5), 100 mM NH_4Cl, 10 mM $MgCl_2$, 1 mM DTT] plus 25% (v/v)

glycerol at 30°C for 20 min. Various concentrations (0–250 nM) of EF-1α•GTP were incubated together with valylated RNAs (2–5 nM) in EF buffer containing 12.5% glycerol and 0.5 mg/ml fragmented salmon sperm DNA on ice for 15 min (28). The amounts of ternary complex were estimated with a ribonuclease protection/TCA filter precipitation assay (T.W.Dreher, O.C.Uhlenbeck and K.S.Browning, submitted) adapted from Louie *et al.* (29). Binding constants (K_d) were determined computationally from binding curves comprising data from 14 concentrations of EF-1α•GTP, and duplicate binding assays were repeated at least twice. The concentration of EF-1α•GTP was determined from binding experiments in the presence of excess [^{3}H]val-tRNA^{Val} transcript.

3′-adenylation assays

Substrate RNAs (0.2 μM) lacking the 3′-terminal A residues were incubated with the CCA-NTase activity present in the wheat germ aminoacyl-tRNA synthetase preparation in 25 mM Tris–HCl (pH 8.0), 2 mM $MgCl_2$, 0.1 mM spermine and 0.5 mM [α-^{32}P]ATP (1.0–1.5 Ci/mmol) at 30°C. Initial rates were determined by sampling aliquots at 30 s intervals. The aliquots were added to equal volumes of 90% formamide/20 mM EDTA/0.2% xylene cyanol/0.2% bromphenol blue, and stored on ice before boiling for 90 s in preparation for electrophoresis. The denatured samples were separated on 6% polyacrylamide/7 M urea gels, and labelled RNA bands were quantitated using a PhosphorImager (Molecular Dynamics). This gel-based assay suffered from less background interference than did TCA precipitation assays, as mentioned by Yue *et al.* (30). The CCA-NTase activity was present at a concentration (4 μg total protein/ml) in which initial rates were proportional to enzyme concentration.

RESULTS

TYMV RNAs comprising only the TLS are capable of efficient, though not optimal, valylation

Previous studies on the valylation of 3′-fragments of TYMV RNA have shown that aminoacylation kinetics vary with the RNA length (6,31). This variation was at least partly due to the presence of a few 5′-non-viral nucleotides influencing the conformation of the TLS (31). Length effects could also be due to a direct involvement of nucleotides immediately upstream of the TLS in productive interactions with ValRS, as suggested from footprinting studies with yeast ValRS (32), or to the influence of upstream nucleotides in stabilizing the TLS conformation.

Although not directly demonstrated, it has been suggested (19,31) that the 82 nt long TYMV TLS is an autonomous structure capable of high efficiency valylation. To directly answer this question, we compared the valylation profiles of the 6.3 kb TYMV virion RNA, TY-264 RNA (previously named TYSma; 6) and TYMV-TLS RNA. TY-264 is a previously described 3′-fragment of TYMV RNA with 258 3′-nt and 6 heterologous nt (GGGAGA) at the 5′-end; TYMV-TLS RNA is an 83 nt long 3′-fragment of TYMV RNA (shown in Fig. 1) one residue longer than the minimal TLS (the 5′-G residue was present to permit efficient RNA synthesis).

The kinetics of valylation by wheat germ ValRS (Table 2) of TYMV virion RNA, TY-264 and TYMV-TLS RNAs were compared to the valylation of transcripts corresponding to unmodified higher plant (lupine) tRNA^{Val} in two buffer conditions: TM, a low ionic strength buffer (9), and IV, a buffer with 0.1 M potassium acetate and rather low Mg^{2+} and ATP levels that is meant to mimic *in vivo* conditions (11). Taking into account both buffer systems, TY-264 RNA and the tRNA^{Val} transcript were similarly efficient ValRS substrates, while virion RNA was somewhat better and TYMV-TLS somewhat poorer than these RNAs (Table 2). K_m values were little affected by the different reaction conditions, but V_{max} values were 5–20 times lower in IV buffer. Although all three forms of TYMV RNA were efficient substrates for ValRS with V_{max}/K_m values close to those for the tRNA^{Val} transcript, the V_{max}/K_m value increased with length. This higher valylation efficiency of the longer RNAs was more pronounced in IV buffer, in which virion RNA showed a V_{max}/K_m value 22 times that of TYMV-TLS as opposed to 8.2 times in TM buffer; this was largely a K_m effect (Table 2). The influence of RNA length was also evident in the extent of valylation achieved in IV buffer. Non-specific binding to longer RNAs may enhance the initial interception of substrate by ValRS.

Table 2. Valylation of different length TYMV RNAs by wheat germ ValRS

	tRNA^{Val} tr[a]	Virion TYMV RNA[b]	TY-264	TYMV-TLS
TM buffer				
K_m (nM)	86	21	69	225
Rel. V_{max}[c]	1.00	1.96	1.97	2.56
Rel. V_{max}/K_m[c]	1.00	8.03	2.45	0.98
Valylation plateau (mol val/mol RNA)	0.98	1.00	1.02	1.00
IV buffer				
K_m (nM)	34	29	67	196
Rel. V_{max}[c]	0.16	0.37	0.16	0.11
Rel. V_{max}/K_m[c]	0.40	1.10	0.21	0.05
Rel. V_{max}/K_m (IV)[d]	1.00	2.75	0.53	0.12
Effect of buffer on V_{max}/K_m (TM/IV)[e]	2.50	2.92	4.62	19.6
Valylation plateau (mol val/mol RNA)	0.98	1.02	0.34	0.04

[a]Lupine tRNA^{Val} transcript.
[b]Note that virion TYMV RNA lacks the 3′-terminal A residue, but CCA-NTase is present in the wheat germ ValRS preparation.
[c]V_{max} and V_{max}/K_m values are all relative to the values for the lupine tRNA^{Val} transcript determined in TM buffer.
[d]V_{max}/K_m (IV) values are relative to that for lupine tRNA^{Val} transcript determined in IV buffer.
[e]Ratio of V_{max}/K_m determined in TM buffer to V_{max}/K_m determined in IV buffer.
Standard errors are ± 25–30%.
Higher plateau levels could be achieved for the shorter RNAs in IV buffer with higher enzyme levels.

The valylation of other tymoviral TLSs is likewise highly efficient

The high efficiency of TYMV-TLS valylation provided the most convenient basis for studying the valylation of other viral RNAs whose genomic RNAs were not readily available for comparison. We have studied the valylation of the TLSs from two further tymoviruses, kennedya yellow mosaic virus (KYMV) and eggplant mosaic virus (EMV), as well as the TLS from sunn-hemp mosaic tobamovirus (SHMV, also known as the cowpea strain of tobacco mosaic virus, CcTMV). SHMV RNA appears to be a product of natural recombination between the genome of a tobamovirus and the 3′-terminus of a tymovirus (33), and has previously been shown capable of valylation (34). As shown in Figure 1, these TLSs are similar in structure to that of TYMV, although there are numerous sequence differences (reverse shading) and the structure of the acceptor stem pseudoknot of EMV TLS differs from those of the other RNAs. For consistency, KYMV-TLS, EMV-TLS and SHMV-TLS RNAs were provided with a 5′-G beyond the minimal TLS, analogous to TYMV-TLS nucleotide 83.

Table 3 shows that the TYMV TLS is not unique in its ability to be highly efficiently valylated. V_{max}/K_m values in TM buffer were very similar for the KYMV, EMV, SHMV and TYMV TLSs and the $tRNA^{Val}$ transcript; KYMV and EMV TLSs had V_{max}/K_m values only ~3–4-fold lower than that of $tRNA^{Val}$ in IV buffer. As for the TYMV RNAs, the lower valylation efficiencies of the KYMV and EMV TLSs in IV buffer were a consequence of lower V_{max} values. SHMV-TLS was very poorly valylated in IV buffer, and this reaction was not kinetically characterized; it is perhaps noteworthy that this is the only RNA studied with a C, rather than A, discriminator base (nt 4). This nucleotide contributes to the valine identity of TYMV RNA towards yeast ValRS (35), and perhaps towards wheat germ ValRS in IV buffer, though clearly not in TM buffer.

Table 3. Valylation of viral TLSs and $tRNA^{Val}$ transcript by wheat germ ValRS

	$tRNA^{Val}$ tr[a]	TYMV-TLS	KYMV-TLS	EMV-TLS	SHMV-TLS
TM buffer					
K_m (nM)	86	225	66	105	60
Rel. V_{max}	1.00	2.56	0.82	2.25	0.61
Rel. V_{max}/K_m	1.00	0.98	1.07	1.84	0.88
IV buffer					
K_m (nM)	34	196	55	143	nd[b]
Rel. V_{max}	0.16	0.11	0.08	0.19	nd[b]
Rel. V_{max}/K_m	0.40	0.05	0.13	0.11	nd[b]

Standard errors are ± 25–30%. V_{max} and V_{max}/K_m values are all relative to the values for the lupine $tRNA^{Val}$ transcript determined in TM buffer.
[a]Lupine $tRNA^{val}$ transcript.
[b]nd, not determined, due to very low rates.

Low-level histidine identity is a background characteristic of tymoviral TLSs

We have previously reported that 3′-fragments of TYMV RNAs can be substantially charged with histidine by purified yeast histidyl-tRNA synthetase (HisRS) (36). To probe whether histidylation might be efficient enough to play a role in TYMV biology, the RNAs listed in Tables 2 and 3 were subjected to histidylation by both the HisRS activity present in our wheat germ aminoacyl-tRNA synthetase preparation and by pure yeast HisRS. No histidine charging that was reliably above background was detected in TM or IV buffers when using wheat germ HisRS (13 μg total protein/ml), although a lupine $tRNA^{His}$ transcript (23) was fully histidylated (not shown).

Substrate levels of yeast HisRS were, however, capable of substantial histidylation of some of the RNAs. For TYMV RNA, the TLS form was a better substrate than the longer forms (Table 4A). The extent of histidylation was strongly dependent on HisRS concentration, with appreciable plateau levels requiring a concentration similar to that of the RNA (Table 4B). TLSs from TYMV, KYMV and SHMV were similarly histidylated, but much lower plateau levels were observed for EMV-TLS (Table 4A).

Table 4.

(**A**) Comparison of RNAs

RNA	Plateau level (mol his/mol RNA)[a]
$tRNA^{His}$ tr[b]	1.18
virion TYMV RNA	0.08[c]
TY-264	0.35[c]
TYMV-TLS	0.46
KYMV-TLS	0.57
EMV-TLS	0.08
SHMV-TLS	0.48

[a]RNAs (100 nM) were incubated with 90 nM yeast HisRS in TM buffer containing 10 μM [^{3}H]histidine for 80 min at 30°C. Mean of two determinations. Somewhat higher levels of histidylation could be achieved for the viral RNAs in H2 buffer: 25 mM Tris–HCl (pH 8.5), 7.5 mM $MgCl_2$, 0.5 mM ATP (36).
[b]Lupine $tRNA^{His}$ *in vitro* transcript.
[c]Plateau not reached at 80 min.

(**B**) Effect of HisRS concentration on histidylation of TYMV-TLS (100 nM)

His RS concentration (nM)	Plateau level (mol his/mol RNA)	
	TM buffer	IV buffer
180	0.49	0.32
90	0.38	0.16
18	0.10	0.09

Reaction conditions were as in Table 2.

Derivatives of TY-264 RNA with anticodons CGC or GUG replacing the wild type CAC or with a CCCAUCA anticodon loop replacing the wild type CCCACAC sequence were histidylated to similar or somewhat higher plateau levels than TY-264 RNA in assays like those of Table 4A (not shown). TYMV genomes bearing these mutations are all non-viable (10). There is thus no

correlation between the histidylation capacity of the viral RNA and replication, while such a correlation exists for valylation capacity (10). Together with the absence of histidylation by catalytic levels of plant histidyl-tRNA synthetase, we conclude that the histidine acceptance of TYMV RNA is unlikely to play a role in viral biology.

The valylatable viral TLSs exhibit a range of EF-1α•GTP binding affinities

Viral RNAs and the $tRNA^{Val}$ transcript were preparatively valylated with [^{3}H]valine and incubated in binding reactions with activated wheat germ EF-1α•GTP. The formation of ternary complex (aminoacyl-tRNA/EF-1α/GTP) was followed in a ribonuclease protection assay as the amount of TCA-precipitable [^{3}H]valine after ribonuclease treatment: the binding of EF-1α•GTP protects the normally accessible 3′-end against ribonuclease attack. Binding constants were determined from binding curves in which the concentration of active EF-1α•GTP varied in 2-fold dilutions from 200 to 0.05 nM. The valylated $tRNA^{Val}$ transcript and three forms of valylated TYMV RNA (virion RNA, TY-264 and TYMV-TLS) all formed tight complexes with EF-1α•GTP, with K_d values between 1.8 and 2.3 nM (Table 5).

Table 5. Binding constants for the interaction of valylated RNAs with wheat germ EF-1α•GTP

RNA	K_d (nM)[a]
val-$tRNA^{Val}$ (transcript, lupine)	2.3 ± 0.4
val-TYMV RNA (virion genomic)	1.8 ± 0.4
val-TY-264	1.9 ± 0.4
val-TYMV-TLS	2.0 ± 0.3
val-KYMV-TLS	2.4 ± 0.3
val-EMV-TLS	57 ± 16[b]
val-SHMV-TLS	9.0 ± 1.3

[a]± indicates standard error.
[b]Determined by competition assay.

Table 6. 3′-Adenylation of -CC 3′-RNAs by wheat germ CCA-NTase

RNA[a]	Rel. rate[b]
$tRNA^{Val}$ (tr, lupine)	1.00
TYMV RNA (virion genomic)	0.59 ± 0.24
TYMV-TLS	0.71 ± 0.22
KYMV-TLS	0.46 ± 0.15
EMV-TLS	1.27 ± 0.66
SHMV-TLS	1.04 ± 0.09

[a]RNAs with 3′-CC termini were made as transcripts from appropriate PCR-generated templates; TYMV virion RNAs have predominantly 3′-CC termini (18).
[b]Initial rates determined at 0.2 μM RNA and 0.5 mM [^{32}P]ATP in TM buffer at 30°C with partially purified wheat germ CCA-NTase at 4 μg protein/ml; rates are expressed relative to that for $tRNA^{Val}$ (3′-CC). ± indicates standard error.

Valylated KYMV-TLS RNA also formed a high-affinity complex (K_d = 2.4 nM), while valylated SHMV-TLS RNA bound EF-1α•GTP with 4–5-fold lower affinity than the other RNAs (Table 5). Valylated EMV-TLS RNA formed even weaker complexes; with the EF-1α•GTP concentrations available to us, the binding curves were incomplete, only ~15% of the val-EMV-TLS RNA forming ternary complexes. This value was between 50 and 80% for the other RNAs in Table 5, all of which reached binding plateaus; the deviation from 100% presumably indicates the presence of some inactive, possibly denatured, RNA in the assays.

The affinity of val-EMV-TLS binding to EF-1α•GTP was estimated in a competition variant of the binding assay, using [^{35}S]methionine-$tRNA^{Met}$ transcript as the reporter. This approach yielded a K_d of 57 nM (Table 5), 25-fold higher than for the $tRNA^{Val}$ transcript. Since the competition approach yields high errors, it will be useful to determine the K_d for val-EMV-TLS binding directly when higher concentrations of EF-1α are available. To test whether EMV-TLS RNA is unusually sensitive to exposure to phenol/chloroform or ethanol, encountered during routine preparation of [^{3}H]valylated RNAs for binding assays, we also prepared [^{3}H]val-EMV-TLS RNA using pure yeast ValRS. This permitted the valylated RNA to be used directly in binding assays without further manipulation. No differences in binding behavior were observed.

CCA-NTase substrate activity of the viral RNAs

Variants of $tRNA^{Val}$ and the viral TLSs lacking the 3′-terminal adenylate were compared as substrates for wheat germ CCA-NTase, present in the aminoacyl-tRNA synthetase preparation. Initial rates at 0.2 μM RNA concentration were determined by measuring the incorporation of [α-^{32}P]ATP using a gel electrophoretic assay. Due to the high K_m(ATP) for CCA-NTases (37), the ATP concentration was 0.5 mM. Activity in TM buffer differed little from activity in the more alkaline buffers typical of CCA-NTase assays (37,38). Table 6 compares the initial rates obtained in TM buffer for the six RNAs studied. The rates for the viral RNAs are within a factor of two of the rate for the $tRNA^{Val}$ transcript.

Erysimum latent virus contrasts by possessing only minimal tRNA mimicry

Although TYMV-like TLSs are typical of tymoviral RNAs (21), erysimum latent virus (ELV) is an exception. On the basis of the biology of the virus and its genomic sequence (22), ELV is clearly a tymovirus. Figure 1 shows the predicted folding of the 3′-97 nt of the 3′-adenylated form of the viral RNA; this encompasses the entire 3′-non-coding region of the RNA. We have recently observed that a chimeric TYMV genome in which the TYMV TLS was replaced with the ELV sequences shown in Figure 1 is infectious (12). Since we did not have ELV virion RNA on hand, our studies used this chimeric RNA, both the full-length progeny virion RNA (named TYMC-H; 12) and a short 3′-fragment of this chimeric RNA, TY-ELV, a 275 nt long chimeric variant of TY-264. Structure predictions found no tRNA-like structural elements in the coding region upstream of the 3′-97 nt of ELV RNA, and the viability of the chimeric genome bearing these limited ELV sequences suggests that they are a functional entity, and that they are appropriately folded in the chimeric context.

We have previously conducted exhaustive tests to identify aminoacylation activity of TYMC-H virion or TY-ELV RNAs using our wheat germ aminoacyl-tRNA synthetase extract, and detected no charging among 13 aminoacylation specificities shown to be active, including valine and histidine (12). We have

now re-examined the histidine identity of two forms of TY-ELV RNA using high concentrations of yeast HisRS: TY-ELV-CCCCA, which has the ELV sequence shown in Figure 1, and TY-ELV-CCCA, which has one less C residue adjacent to the 3′-A and so has the same 3′-sequence as progeny TYMC-H RNA (12). Both forms of TY-ELV RNA could be histidylated to 0.4–0.5 mol histidine/mol RNA (100 nM RNA, 180 nM HisRS, TM buffer), and were thus similar to the viral TLS RNAs studied in Table 4A (except EMV-TLS) as substrates for yeast HisRS.

Although the lack of efficient aminoacylation seemed to preclude high-affinity interaction with EF-1α•GTP, we did use a competition variant of our EF-1α binding assay to test whether TY-ELV-CCCCA or TY-ELV-CCCA RNAs were capable of forming unusual tight complexes in the absence of aminoacylation. No decrease in ternary complex formation of reporter [^{35}S]methionine-tRNA^{Met} was observed in the presence of 500-fold higher concentrations of the TY-ELV RNAs.

Finally, the 3′-adenylation of TYMC-H virion RNA (verified as having predominantly 3′-CC termini) was examined. In experiments parallel to those reported in Table 6, we were unable to determine the initial rate of 3′-adenylation due to low activity (estimated to be <0.01% that for TYMC RNA). We have previously reported (12) that TYMC-H RNA incorporated about 15% the amount of [α-^{32}P]ATP incorporated by TYMV RNA in TM buffer containing 0.1 mM ATP and 0.1 μM RNA in a 20 min reaction at 30°C with wheat germ CCA-NTase.

DISCUSSION

TYMV RNA and tRNA^{Val} have closely similar activity in three properties

Comparison to the valylation of a higher plant tRNA^{Val} transcript showed that the valylation efficiencies (V_{max}/K_m) and Michaelis constants (V_{max} and K_m) of TYMV RNA were all close to those of the tRNA (Tables 2 and 3). Interestingly, comparison of the valylation efficiencies of different lengths of TYMV RNA showed that the valylation of full-length (6219 nt) virion (3′-CCA) RNA was superior to shorter forms, and even better than the tRNA^{Val} transcript; V_{max}/K_m values are often only some 5-fold lower for *in vitro*-transcribed tRNAs compared to their fully modified counterparts (25,39,40). The valylation efficiency we have determined with plant ValRS is considerably higher than that determined with the non-homologous yeast ValRS (5). From our results, it is hardly surprising that TYMV RNAs can be valylated *in vivo* (7,8). Similarly efficient valylation was also observed for KYMV and EMV RNAs. This astounding degree of tRNA mimicry applies equally well to interaction with EF-1α (for TYMV and KYMV RNAs; Table 5) and to 3′-adenylation by CCA-NTase of 3′-CC RNAs (for TYMV, KYMV, EMV and SHMV RNAs; Table 6). One may confidently conclude that valylation, EF-1α interaction and 3′-adenylation by CCA-NTase occur *in vivo* and are likely to play roles in the life cycles of some of the tymoviruses.

In view of significant deviation from the features present in canonical tRNAs, it is interesting that the tymoviral RNAs are such excellent tRNA mimics. The presence of the acceptor stem pseudoknot is apparently very compatible with the normal protein/tRNA interactions. This is explained by the recent determination of the NMR structure of the acceptor/T arm of TYMV RNA as a colinear stack of three A-form helices, with the pseudoknot loops L1 and L2 residing within the grooves of the helix (41). The viral RNAs also show that some differences in invariant nucleotides are compatible with efficient tRNA function. The EMV and SHMV RNAs have purines in the 5′ part of the anticodon loop, where canonical tRNAs exclusively have pyrimidines, yet especially EMV-TLS RNA was an excellent substrate for ValRS (Table 3), the most likely of the three functions we studied to be affected. These conclusions are corroborated by the observation that a C to A substitution in the 5′-most nucleotide of the anticodon loop of yeast tRNA^{Thr} did not alter the kinetic parameters of threonylation (40). The tymoviral RNAs also deviate from the conserved tRNA sequences in the D-loop (no GG dinucleotide) and T-loop [no UUC(G/A), which becomes modified to TΨC(G/A)]. The conserved G19:C56 and G18:U55 basepairs of tRNAs may be mimicked by a G75:C36 basepair and replaced by an A76:G37 basepair, respectively, in the TYMV and related TLSs (Fig. 1). This unusual pairing is compatible with high efficiency valylation and EF-1α•GTP interaction. Similarly, mutant *E.coli* tRNA^{Phe} with the corresponding non-canonical A18:G55 base pair has been shown to have the same k_{cat}/K_m for aminoacylation and K_d for EF-Tu•GTP binding as the wild type tRNA (42). Apart from its crucial role in overall tRNA conformation through its interaction with the D-loop, the T-loop is also close to the site of interaction with EF-Tu (43) and presumably EF-1α, and is apparently directly contacted by CCA-NTases (44,45). CCA-NTases from yeast and *E.coli* require a purine at nucleotide 57 in the T-loop of tRNA, a position equivalent to nucleotide 35 of TYMV RNA; this position is occupied by a purine in the TYMV, KYMV, EMV and SHMV TLSs (Fig. 1), all of which are excellent CCA-NTase substrates (Table 6).

Our kinetic analyses of the length effects on the tRNA mimicry of TYMV RNA showed that, although the TLS itself is an autonomous element capable of remarkable tRNA mimicry, the 6.3 kb virion RNA is a considerably better substrate for ValRS. No length advantage is apparent in ternary complex formation with EF-1α•GTP (Table 5), nor in 3′-adenylation by CCA-NTase (Table 6), both functions which are thought to primarily involve interaction with the acceptor/T arm. This suggests that the presence of upstream sequences has little effect on acceptor/T arm conformation, but may stabilize the overall TLS L-conformation. Genetic interaction indicated by phenotypic interdependence (46) between TYMV nucleotides 53 and 96 (numbered from the 3′-end) suggests a candidate interaction of this type. Alternatively, there may be helpful productive contacts between upstream sequences and ValRS, as suggested by protection experiments with yeast ValRS showing interaction immediately upstream of the TLS (32). Neither of the above considerations addresses the significant advantage of the virion RNA over TY-264, however; the low K_m for virion RNA suggests that the large bulk of RNA may enhance initial ValRS binding.

Distinct properties associated with two types of acceptor/T arm

The acceptor/T arms of tymoviral TLSs are built on at least two structural formats. For TYMV (and KYMV and SHMV) RNAs, this arm is built of three coaxial stacked helical segments 4, 3 and 5 bp in length (the latter two segments comprising the pseudoknot), with pseudoknot loop L1 containing 4 nt (Fig. 1). By contrast, the EMV acceptor/T arm is built of stacked 3, 3 and 6 bp segments, with L1 containing only two nucleotides.

The tRNA mimicry of TYMV and KYMV RNAs is extremely efficient, these RNAs supporting high rates of valylation and 3′-adenylation, as well as forming tight complexes with EF-1α•GTP (Tables 2, 3 and 5). EMV RNA was as efficient as these RNAs in valylation (Table 3) and 3′-adenylation (Table 6), but differed from these RNAs in two characteristics: EMV RNA bound EF-1α•GTP more weakly (Table 5; K_d of 57 nM compared with ~2 nM), and could be histidylated with high concentrations of yeast HisRS to only 0.08 mol histidine/mol RNA, a plateau some 5-fold lower than those for TYMV and KYMV RNAs (Table 4A). The results of a parallel study with furoviral RNAs that contain tymoviral-like TLSs (47) corroborate the above differences in the properties of TLSs with the two types of acceptor/T arm. Thus, all RNAs with a 4:3:5 bp arm (including soil-borne wheat mosaic and beet soil-borne furovirus RNAs) have highly developed tRNA mimicry, while both RNAs that we have tested with a 3:3:6 bp arm (EMV and potato mop-top furovirus RNAs) are markedly less efficient in EF-1α•GTP interaction and histidylation. We believe this relates to differences in the conformation of the acceptor/T arm, along which EF-Tu (43), and presumably EF-1α, interacts and which includes the major histidine identity elements at the acceptor end of the helix (48). The different segment lengths in the pseudoknot, as well as the presence of only 2 nt in loop L1, probably result in the loss of a stacked nucleotide opposite the discriminator base (nt 4; numbering from 3′-end). The two nucleotides from loop L1 that were found to be stacked in this position in the NMR structure of the TYMV acceptor/T arm (41) are probably responsible for this RNA's partial histidine identity (48). Note that although TYMV and other tymoviral RNAs are capable of histidylation, histidine charging to appreciable levels is dependent on substrate levels of HisRS, and represents only a background identity in comparison to the highly efficient valylation.

Tymoviral tRNA mimicry ranges from highly efficient to vestigial

Given the clear importance of the role of aminoacylation in the biology of TYMV (10,11), it has been surprising to discover that tRNA mimicry covers a wide range across the tymovirus group. Some of that range arises due to the presence of the different acceptor/T arm formats discussed above. The range is greatly widened, however, by the properties of ELV RNA, which has no valine identity and no apparent TLS except for an extra-long acceptor/T arm analogue. ELV RNA shares the background histidine identity common to the TYMV-type RNAs, but is only a poor substrate for CCA-NTase. The 3′-terminus of ELV RNA has similarities to the tobacco rattle tobravirus RNA 3′-terminus (49), but no other tymoviral or furoviral examples are known.

Our motivation in designing these studies was the goal of understanding the role of tRNA mimicry in viral biology. Discovering that great diversity of tRNA mimicry exists within the tymoviruses suggests that whatever the major function(s) provided by the highly developed TYMV-type TLS is, that function is not strongly fixed evolutionarily, and can be provided rather easily in other ways. This in turn suggests that the major TLS function is mechanistically simple, not involving multiple interactions with other viral components. TLS function is clearly crucial in TYMV (10,11), yet the TYMV TLS can be replaced with the ELV 3′-non-coding region to produce an infectious chimeric RNA (12). These dissimilar termini evidently provide a similar function, though presumably through interactions with different host proteins. A possible major function of the 3′-terminus is to permit regulated switching of access by the viral RNA polymerase to the minus strand initiation site opposite the 3′-most C residue (50). Decreased initiation site access might be achieved for TYMV RNA after binding EF-1α•GTP, while some other protein must play this role for ELV. Yet another protein may be involved in the case of EMV, depending on the extent to which the weak EF-1α binding will permit complex formation *in vivo*.

The diversity of tRNA mimicry seen within the tymoviruses is perhaps general among the groups of plant viruses with aminoacylatable RNAs. We have recently shown this to be the case for the furoviruses (47), and it has been reported that tomato aspermy cucumovirus RNA cannot be tyrosylated, in contrast to cucumber mosaic cucumovirus RNA (51). Such diversity within viral genera indicates that changes in tRNA mimicry do not represent large evolutionary steps. Indeed, the closest relatives of the tymoviruses are the marafiviruses, whose RNAs have a poly(A) tail (52), while alfalfa mosaic virus, whose RNAs have 3′-termini without a TLS or poly(A) tail, but which must be bound at the 3′-end by coat protein to initiate an infection (53), is closely related to the bromo- and cucumoviruses, whose RNAs are tyrosylatable (54).

ACKNOWLEDGEMENTS

We thank Dr Karen Browning for the gift of wheat germ EF-1α, Drs Richard Giegé and Catherine Florentz for the gifts of purified yeast valyl- and histidyl-tRNA synthetase, and Dr Shigeo Yoshinari for help with the manuscript. These studies were supported by grants from NIH (AI-33907 and GM-54610). This is technical report No. 11294 of the Oregon Agricultural Experiment Station.

REFERENCES

1 Haenni,A.-L., Joshi,S. and Chapeville,F. (1982) *Prog. Nucl. Acid Res. Mol. Biol.*, **27**, 85–104.
2 Mans,R.M., Pleij,C.W. and Bosch,L. (1991) *Eur. J. Biochem.*, **201**, 303–324.
3 Pinck,M., Yot,P., Chapeville,F. and Duranton,H.M. (1970) *Nature*, **226**, 954–956.
4 Yot,P., Pinck,M., Haenni,A.-L., Duranton,H.M. and Chapeville,F. (1970) *Proc. Natl Acad. Sci. USA*, **67**, 1345–1352.
5 Giegé,R., Briand,J.-P., Mengual,R., Ebel,J.-P. and Hirth,L. (1978) *Eur J. Biochem.*, **84**, 251–256.
6 Dreher,T.W., Florentz,C. and Giegé,R. (1988) *Biochimie*, **70**, 1719–1727.
7 Joshi,S., Haenni,A.-L., Hubert,E., Huez,G. and Marbaix,G. (1978) *Nature*, **275**, 339–341.
8 Joshi,S., Chapeville,F. and Haenni,A.-L. (1982) *EMBO J.*, **1**, 935–938.
9 Dreher,T.W., Tsai,C.-H., Florentz,C. and Giegé,R. (1992) *Biochemistry*, **31**, 9183–9189.
10 Tsai,C.-H. and Dreher,T.W. (1991) *J. Virol.*, **65**, 3060–3067.
11 Dreher,T.W., Tsai,C.-H. and Skuzeski,J.M. (1996) *Proc. Natl Acad. Sci. USA*, **93**, 12212–12216.
12 Goodwin,J.B., Skuzeski,J.M. and Dreher,T.W. (1997) *Virology*, **230**, 113–124.
13 Singh,R.N. and Dreher,T.W. (1998) *RNA*, **4**, 1083–2095.
14 Pallanck,L., Pak,M. and Schulman,L.H. (1995) In Söll,D. and RajBhandary,U.L. (eds), *tRNA: Structure, Biosynthesis and Function.* ASM Press, Washington, DC, pp. 371–394.
15 Joshi,R.L., Faulhammer,H., Chapeville,F., Sprinzl,M. and Haenni,A.-L. (1984) *Nucleic Acids Res.*, **12**, 7467–7478.
16 Litvak,S., Tarrago,A., Tarrago-Litvak,L. and Allende,J.E. (1973) *Nature New Biol.*, **241**, 88–90.
17 Joshi,R.L., Ravel,J.M. and Haenni,A.-L. (1986) *EMBO J.*, **5**, 1143–1147.
18 Briand,J.-P., Jonard,G., Guilley,H., Richards,K. and Hirth,L. (1977) *Eur. J. Biochem.*, **72**, 453–463.

19 Joshi,S., Chapeville,F. and Haenni,A.-L. (1982) *Nucleic Acids Res*., **10**, 1947–1962.
20 Pinck,M. and Hall,T.C. (1978) *Virology*, **88**, 281–285.
21 van Belkum,A., Bingkun,J., Rietveld,K., Pleij,C.W.A. and Bosch,L. (1987) *Biochemistry*, **26**, 1144–1151.
22 Srifah,P., Keese,P., Weiller,G. and Gibbs,A. (1992) *J. Gen. Virol*., **73**, 1437–1447.
23 Skuzeski,J.M., Bozarth,C.S. and Dreher,T.W. (1996) *J. Virol*., **70**, 2107–2115.
24 Tsai,C.-H. and Dreher,T.W. (1993) *BioTechniques*, **14**, 58–61.
25 Sampson,J.R. and Uhlenbeck,O.C. (1988) *Proc. Natl Acad. Sci. USA*, **85**, 1033–1037.
26 Barciszewska,M. and Jones,D.S. (1987) *Nucleic Acids Res*., **15**, 1333.
27 Lax,S.R., Lauer,S.J., Browning,K.S. and Ravel,J.M. (1986) *Methods Enzymol*., **118**, 109–128.
28 Nagata,S., Iwasaki,K. and Kaziro,Y. (1976) *Arch. Biochem. Biophys*., **172**, 168–177.
29 Louie,A., Ribeiro,N.S., Reid,B.R. and Jurnak,F. (1984) *J. Biol. Chem*., **259**, 5010–5016.
30 Yue,D., Maizels,N. and Weiner,A.M. (1996) *RNA*, **2**, 895–908.
31 Mans,R.M.W., Verlaan,P.W.G., Pleij,C.W.A. and Bosch,L. (1990) *Biochim. Biophys. Acta*, **1050**, 186–192.
32 Florentz,C. and Giegé,R. (1986) *J. Mol. Biol*., **191**, 117–130.
33 Meshi,T., Ohno,T., Iba,H. and Okada,Y. (1981) *Mol. Gen. Genet*., **184**, 20–25.
34 Beachy,R.N., Zaitlin,M., Bruening,G. and Israel,H.W. (1976) *Virology*, **73**, 498–507.
35 Florentz,C., Dreher,T.W., Rudinger,J. and Giegé,R. (1991) *Eur. J. Biochem*., **195**, 229–234.
36 Rudinger,J., Florentz,C., Dreher,T. and Giegé,R. (1992) *Nucleic Acids Res*., **20**, 1865–1870.
37 Deutscher,M.P. (1982) *tRNA Nucleotidyltransferase. The Enzymes*, **XV**, 183–215.
38 Shanmugam,K., Hanic-Joyce,P.J. and Joyce,P.B.M. (1996) *Plant Mol. Biol*., **30**, 281–295.
39 Jahn,M., Rogers,M.J. and Söll,D. (1991) *Nature*, **352**, 258–260.
40 Nameki,N. (1995) *Nucleic Acids Res*., **23**, 2831–2836.
41 Kolk,M.H., van der Graaf,M., Wijmenga,S.S., Pleij,C.W.A., Heus,H.A. and Hilbers,C.A. (1998) *Science*, **280**, 434–438.
42 Peterson,E.T., Blank,J., Sprinzl,M. and Uhlenbeck,O.C. (1993) *EMBO J*., **12**, 2959–2967.
43 Nissen,P., Kjeldgaard,M., Thirup,S., Polekhina,G., Reshetnikova,L., Clark,B.F.C. and Nyborg,J. (1995) *Science*, **270**, 1464–1472.
44 Hegg,L.A. and Thurlow,D.L. (1990) *Nucleic Acids Res*., **18**, 5975–5979.
45 Li,Z., Gillis,K.A., Hegg,L.A., Zhang,J. and Thurlow,D.L. (1996) *Biochem. J*., **314**, 49–53.
46 Tsai,C.-H. and Dreher,T.W. (1992) *J. Virol*., **66**, 5190–5199.
47 Goodwin,J.B. and Dreher,T.W. (1998) *Virology*, **246**, 170–178.
48 Rudinger,J., Felden,B., Florentz,C. and Giegé,R. (1997) *Bioorg. Med. Chem*., **5**, 1001–1009.
49 van Belkum,A., Cornelissen,B., Linthorst,H., Bol,J., Pleij,C. and Bosch,L. (1987) *Nucleic Acids Res*., **15**, 45–58.
50 Singh,R.N. and Dreher,T.W. (1997) *Virology*, **233**, 430–439.
51 Joshi,R.L. and Haenni,A.-L. (1986) *FEBS Lett*., **194**, 157–160.
52 Edwards,M.C., Zhang,Z. and Weiland,J.J. (1997) *Virology*, **232**, 217–229.
53 Houwing,C.J. and Jaspars,E.M. (1978) *Biochemistry*, **17**, 2927–2933.
54 Koonin,E.V. and Dolja,V.V. (1993) *CRC Crit. Rev. Biochem. Mol. Biol*., **28**, 375–430.